ELECTRONIC SUPPLEMENTARY INFORMATION

Preparation and in-system study of SnCl$_2$ precursor layers: Towards vacuum-based synthesis of Pb-free perovskites

Roberto Félix,[1] Núria Llobera-Vila,[1] Claudia Hartmann,[1] Carola Klimm,[1] Dan R. Wargulski,[1] Manuel Hartig,[1,2] Regan G. Wilks,[1,3] and Marcus Bär[1,3]

[1]*Renewable Energy, Helmholtz-Zentrum Berlin für Materialien und Energie GmbH, Hahn-Meitner-Platz 1, D-14109 Berlin, Germany*

[2] *Technologie für Dünnschicht-Bauelemente, Technische Universität Berlin - Fak. IV, HFT 5-2, Einsteinufer 25, D-10587 Berlin, Germany*

[3]*Energy Materials In-Situ Laboratory Berlin (EMIL), Helmholtz-Zentrum Berlin für Materialien und Energie GmbH, Albert-Einstein-Straße 15, D-12489 Berlin, Germany*
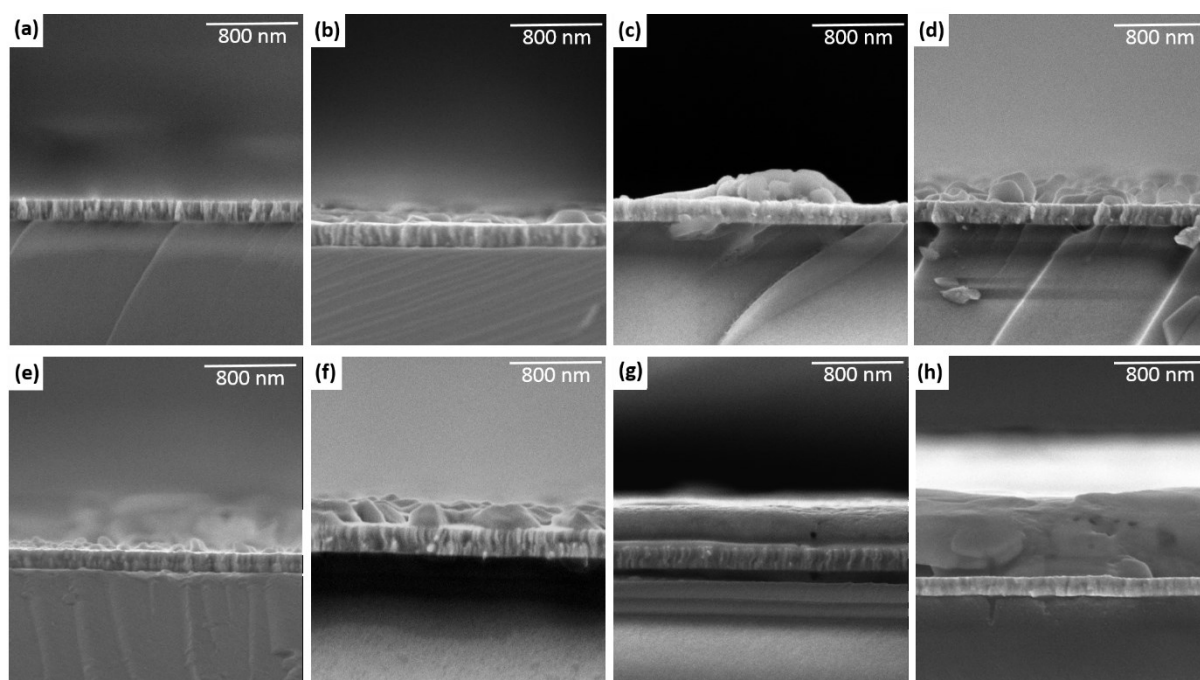
Fig. S1: Cross section scanning electron microscope (SEM) images of SnCl$_2$/Mo samples with the following SnCl$_2$ evaporation times: (a) 25 s, (b) 50 s, (c) 100 s, (d) 200 s, (e) 400 s, (f) 600 s, (g) 800 s, and (h) 1600 s. The SEM images were taken with a 30,000× magnification.

Fig. S1 presents cross section scanning electron microscope (SEM) images of the investigated sample series. The SEM images of samples with evaporation treatments between 100 s and 400 s (and especially for the "200 s" sample) show that the deposited SnCl$_2$ islands grow vertically, with maximum heights of ca. 150 ± 25 nm, which leave a large substrate area uncovered. With longer evaporation treatments (e.g., "400 s" and "600 s" samples), the islands begin to grow laterally and to cover a greater substrate area, maintaining their peak heights unchanged. Once the islands coalesce (e.g., "800 s" and "1600 s" samples), the SnCl$_2$ film thickness resumes its vertical growth; the thickness of the SnCl$_2$ film for the "1600 s" sample is (715 ± 25) nm.
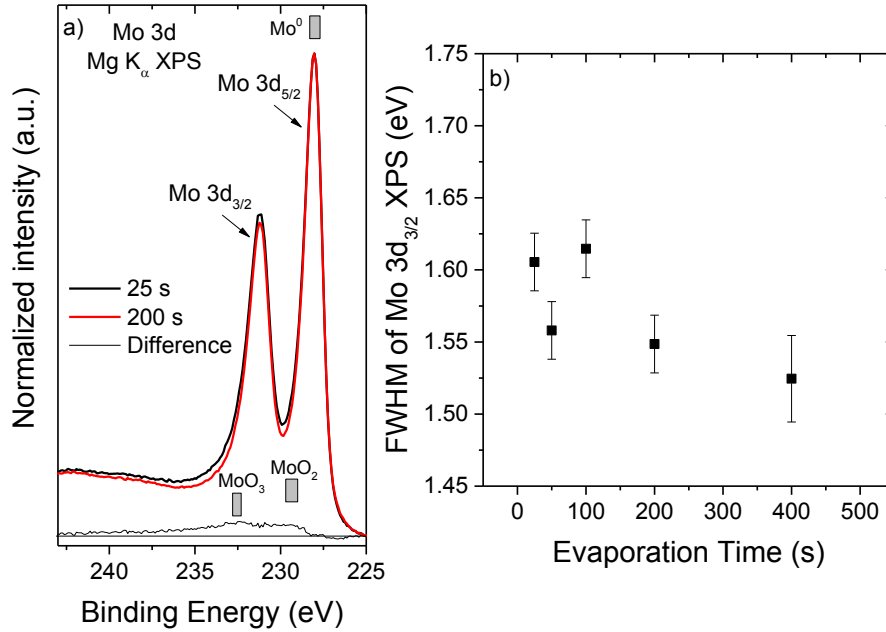
Fig. S2: (a) Detail XPS spectra of the Mo 3d energy region of the sample series, normalized to maximum intensity for shape comparison. The difference line of the spectra (i.e., "25 s" minus "200 s") is also shown. Mo $3d_{5/2}$ binding energy values for reference compounds are denoted by the gray-shaded areas.[1] (b) FWHM values of the Mo $3d_{3/2}$ line of samples produced by evaporation times in the 25 – 400 s range.

Fig. S2 (a) shows that the XPS Mo 3d spectrum of the "25 s" sample has a broader shape line than the spectrum of the "200 s" sample, indicating a higher Mo chemical speciation at the interface with shorter evaporation treatments. This Mo chemical speciation may be a result of O remaining in/on the surface of the Mo-coated substrates (in the form of MoO_x) indicating a not sufficient substrate cleaning and/or the presence of (some) oxygen in the Mo. The difference line of the spectra (i.e., "25 s" minus "200 s") exhibits a shape resembling a broad Mo 3d doublet, as expected of a MoO_x–derived signal. Moreover, the location of the difference signal is found at a higher binding energy (BE) values (compared to the main Mo $3d_{5/2}$ peak of the spectra), which matches BE values Mo $3d_{5/2}$ BE values reported for MoO_2 in literature.[1] (Although an overlapping MoO_3–derived signal cannot be excluded.) Fig. S2 (b) shows the FWHM values of the Mo $3d_{3/2}$ line of samples produced by evaporation times in the 25 – 400 s range. A reduction in FHWM values with evaporation treatment can be seen. These findings suggest a leaching of O from the Mo-coated substrate by the deposited $SnCl_2$ films.

In the following, probable reactions related to the detected O-leaching process are proposed, along with calculations of their respective standard enthalpy of reaction ($\Delta H°_{rxn}$) to give an estimate (i.e., the deposition of $SnCl_2$ thin-films did not take place under standard conditions) of their thermodynamic viability[2]:

$$MoO_2 + 2Sn^0 \rightleftharpoons Mo^0 + 2SnO \qquad (1)$$
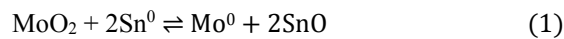
$\Delta H°_{rxn} = \sum \Delta H°_f \text{ (products)} - \sum \Delta H°_f \text{ (reactants)}$, where $\Delta H°_f$ is the standard enthalpy of formation of a compound.

$\Delta H°_{rxn} = [\Delta H°_f (Mo^0) + (2 \text{ mol}) \cdot \Delta H°_f (SnO)] - [\Delta H°_f (MoO_2) + (2 \text{ mol}) \cdot \Delta H°_f (Sn^0)]$

$= [(1 \text{ mol}) \cdot (0 \text{ kJ/mol}) + (2 \text{ mol}) \cdot (-283.26 \text{ kJ/mol})] - [(1 \text{ mol}) \cdot (-543.92 \text{ kJ/mol}) + (2 \text{ mol}) \cdot (0 \text{ kJ/mol})]$

$= -22.6 \text{ kJ/mol}$

Under standard conditions, the reaction is exothermic.

$$MoO_3 + 3Sn^0 \rightleftharpoons Mo^0 + 3SnO \qquad (2)$$
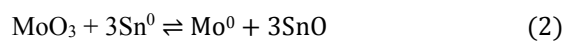
$$\Delta H^\circ_{rxn} = [\Delta H^\circ_f(Mo^0) + (3\ mol) \cdot \Delta H^\circ_f(SnO)] - [\Delta H^\circ_f(MoO_3) + (3\ mol) \cdot \Delta H^\circ_f(Sn^0)]$$

$$= [(1\ mol) \cdot (0\ kJ/mol) + (3\ mol) \cdot (-283.26\ kJ/mol)] - [(1\ mol) \cdot (-754.75\ kJ/mol) + (3\ mol) \cdot (\ 0\ kJ/mol)]$$

$$= -95.0\ kJ/mol$$

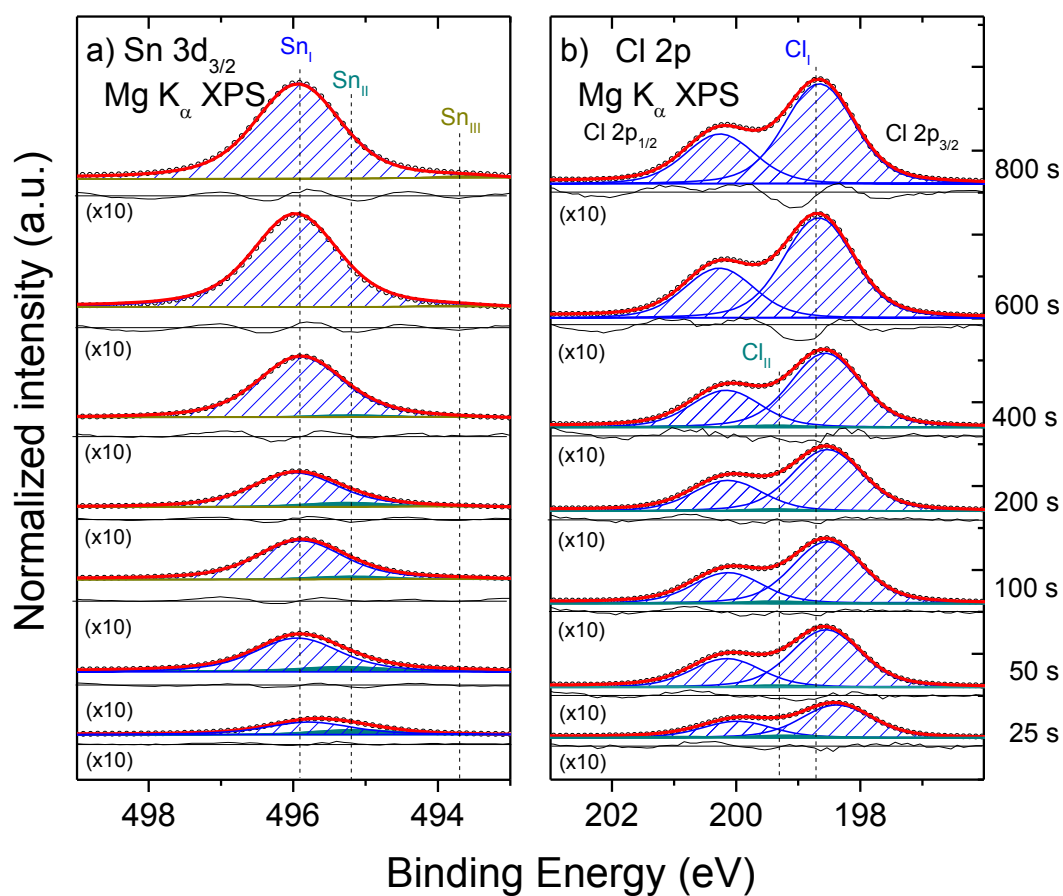Under standard conditions, the reaction is exothermic.

Fig. S3: XPS detail spectra of the (a) Sn $3d_{3/2}$ and (b) Cl 2p energy regions of the investigated sample series, including fits and respective residua. Spectra are normalized to background intensity.
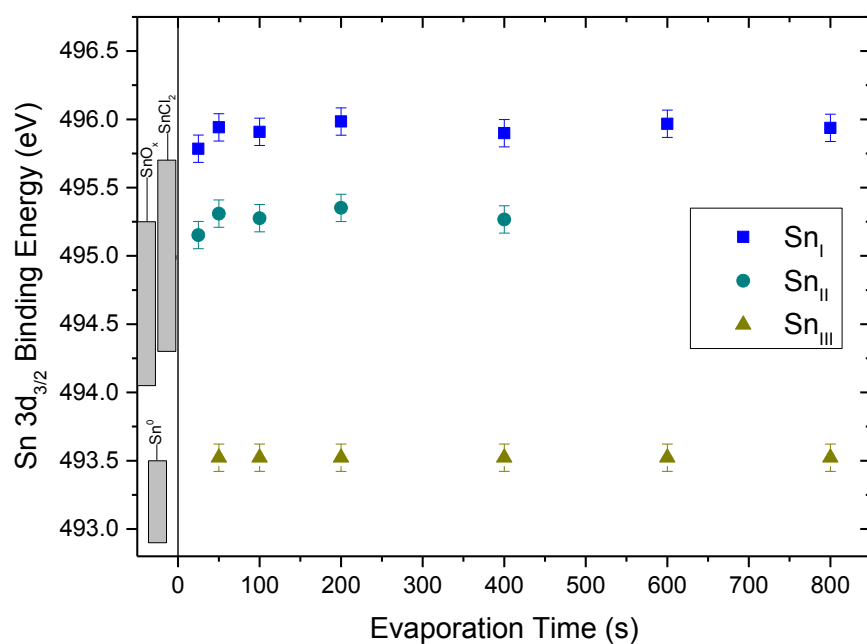
Fig. S4: The binding energy values of the peak contributions of the x-ray photoelectron spectroscopy (XPS) Sn $3d_{3/2}$ spectra of the investigated sample series, presented as a function of evaporation time. The gray-shaded areas denote BE values ranges reported for reference Sn compounds in literature.[1,3-8]

The BE values of the Sn $3d_{3/2}$ peak contributions obtained from the curve fit analysis presented in Fig. S3 (a) are shown in Fig. S4 as a function of evaporation time. BE value ranges for reference Sn compounds (i.e., $SnCl_2$, SnO, SnO_2 and Sn^0) reported in literature are included in the figure.[1,3-8]
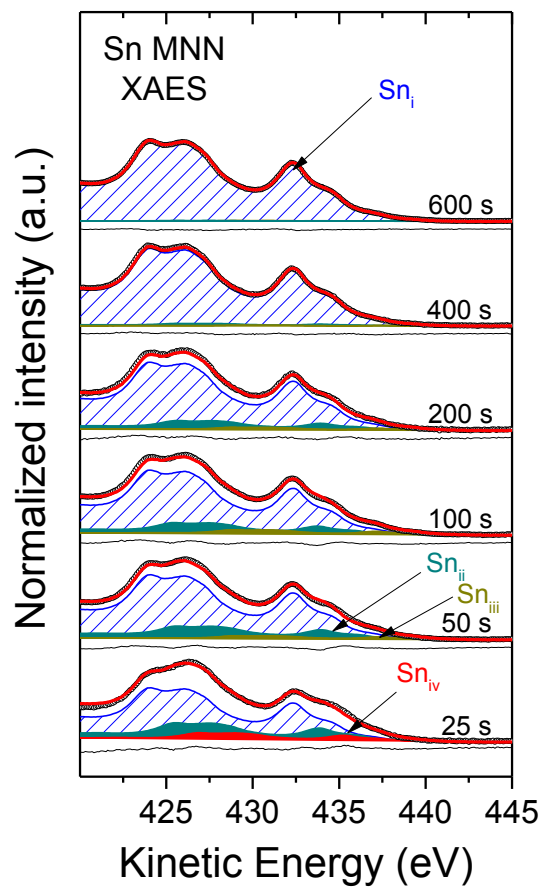
Fig. S5: Curve fit analysis of the Sn MNN spectra of the sample series. Fits of the experimental data have been obtained by adding weighted and energetically shifted contributions of the reference Sn MNN XAES line (i.e., the Sn MNN spectrum of the "800 s" sample).
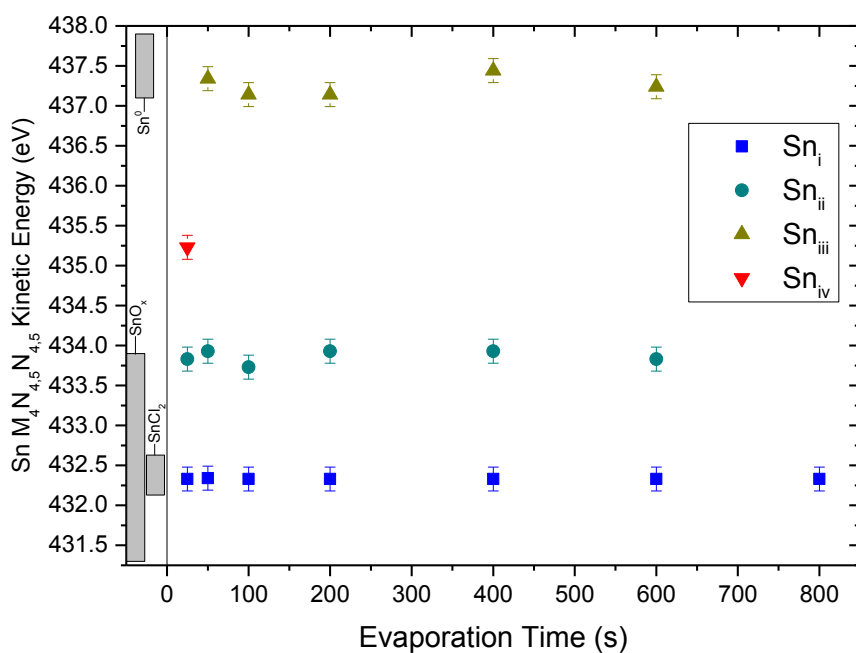
Fig. S6: The kinetic energy values of the components of the x-ray-excited Auger electron spectroscopy (XAES) Sn $M_4N_{4,5}N_{4,5}$ (MNN) spectra of the investigated sample series, presented as a function of evaporation time. The gray-shaded areas denote KE values ranges reported for reference Sn compounds in literature.[1,5-8]

The kinetic energy (KE) values of the components of the Sn $M_4N_{4,5}N_{4,5}$ (MNN) spectra obtained from the curve fit analysis presented in Fig. S5 are shown in Fig. S6 as a function of evaporation time. KE value ranges for reference Sn compounds (i.e., $SnCl_2$, SnO, SnO_2 and Sn^0) reported in literature are included in the figure. [1,5-8]
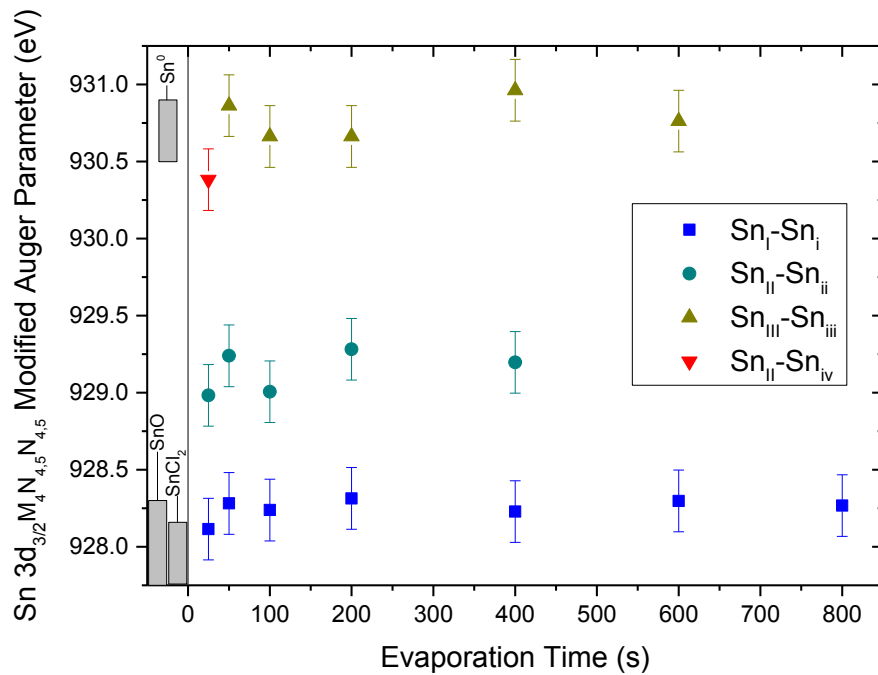
Fig. S7: The Sn modified Auger parameters (α^*) of the investigated sample series, presented as a function of evaporation time. The gray-shaded areas denote Sn (α^*) values ranges reported for reference Sn compounds in literature. [1,5-8]

An analysis of the modified Auger parameters ($\alpha^* = BE_{XPS} + KE_{XAES}$) for the investigated sample series was conducted employing the determined contributions of the XPS Sn $3d_{3/2}$ and the XAES Sn $M_4N_{45}N_{45}$ XAES spectra. Sn α^* values using the Sn_I-Sn_i, Sn_{II}-Sn_{ii}, Sn_{II}-Sn_{iv} and Sn_{III}-Sn_{iii} XPS-XAES line pairs were computed and are shown in Fig. S7 as a function of evaporation time. Sn α^* value ranges for reference Sn compounds (i.e., $SnCl_2$, SnO and Sn^0) reported in literature are included in the figure. [1,5-8]
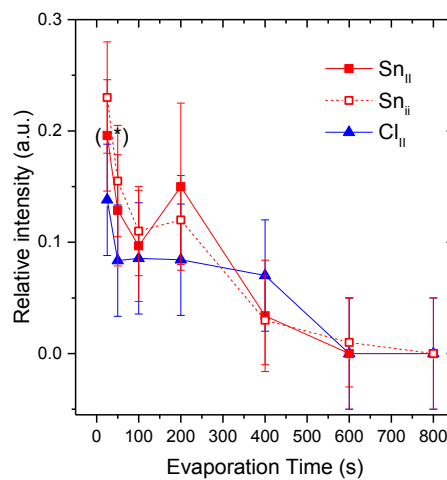

Fig. S8: Relative intensities of the Sn_I, Sn_i and Cl_{II} lines compared to the overall Sn or Cl content as a function of evaporation time.

Fig. S8 shows the relative intensities of the Sn_{II} [i.e., from the curve fit analysis shown in Fig. S3 (a)], Sn_{ii} [i.e., from the curve fit analysis shown in Fig. S5] and Cl_{II} lines [i.e., from the curve fit analysis shown in Fig. S3 (b)] compared to the overall Sn or Cl content throughout the entire sample series. Similar relative intensities as a function of evaporation time are observed for these spectral lines. As discussed in the text, it is highly probable that the Sn_{II} peak of the "25 s" sample is comprised of more than a single Sn chemical species (i.e., two XPS contributions vs three XAES components for the "25 s" sample). To show a more fitting quantification of the predominant Sn chemical species represented by the Sn_{II} contribution, the Sn_{II} value for the "25 s" sample (i.e., 0.29 ± 0.05) was "corrected" by a factor based on the spectral weight of the Sn_{ii} and Sn_{iv} of the curve fit analysis of the XAES Sn MNN spectrum of the "25 s" sample [i.e., $Sn_{ii}/(Sn_{ii} + Sn_{iv}) = (0.23 \pm 0.05)/(0.34 \pm 0.07) = 0.68 \pm 0.07$]. The corrected Sn_{II} value of the "25 s" sample [i.e., $(0.29 \pm 0.05)(0.68 \pm 0.07) = 0.20 \pm 0.7$] is shown in Fig. S8, as indicated by an asterisk.

References

1   J. F. Moulder, W. F. Stickle and P. E. Sobol, *Handbook of X-ray Photoelectron Spectroscopy: A Reference Book of Standard Spectra for Identification and Interpretation of XPS Data*, 2nd ed. Perkin-Elmer, Physical Electronics Division, 1995.
2   F. R. Bichowsky and F. D. Rossini, *Thermochemistry of the Chemical Substances*, Reinhold, New York, 1936.
3   W.-K Choi, H.-J. Jung and S.-K. Koh, *J. Vac. Sci. Technol. A*, 1996, **14**, 359.
4   P. A. Grutsch, M. V. Zeller and T. P. Fehlner, *Inorg. Chem.*, 1973, **12**, 1431.
5   L. Kövér, Z. Kovács, R. Sanjinés, G. Moretti, I. Cserny, G. Margaritondo, J. Pálinkás and H. Adachi, *Surf. Interface Anal.*, 1995, **23**, 461.
6   A. W. C. Lin, N. R. Armstrong, and T. Kuwana, *Anal. Chem.*, 1977, **49**, 1228.
7   L. R. Pederson, *Solar Energy Mater.*, 1982, **6**, 221.
8   C. D. Wagner, L. H. Gale and R. H. Raymond, *Anal. Chem.*, 1979, **51**, 466.